

Optimization of 5-MW wind turbine blade using fluid structure interaction analysis[†]

Dong-Hoon Kim¹, O-Kaung Lim^{2,*}, Eun-Ho Choi² and Yoojeong Noh²

¹Research and Development Center Test and CAE Team, HWASHIN Co. Ltd., Yeongcheon 770-280, Korea

²School of Mechanical Engineering, Pusan National University, Pusan 609-735, Korea

(Manuscript Received April 27, 2015; Revised July 1, 2016; Accepted October 1, 2016)

Abstract

The blade of a wind turbine is a critical component that can be damaged by extreme loads; thus, its structural safety is paramount. Further, because its manufacturing cost comprise a high proportion of overall wind power production cost, its weight should be optimized to save on production and material cost. Much research has been conducted on structural optimization of wind turbine blades; however, focus has only been on exterior design. In this study, we optimize the cross-sectional dimensions of a 5-MW wind turbine blade by performing 3-D fluid analysis of the blade and using the pressure distribution obtained as input loads to find the inner structural shape of its cross section. Subsequent 2-D and 3-D fluid structural analyses conducted to find the maximum stress on the overall blade and its cross sections confirm that the cross section of the blade is minimized and that it is structurally safe.

Keywords: Wind turbine blade; Fluid structure analysis; Topology optimization; Design optimization

1. Introduction

A wind turbine blade is a key component in wind power generation systems. Its rotating motion is converted to electricity and its shape affects the efficiency of the wind generation system in its extraction of energy from the wind. The wind turbine blade is a core part for converting wind pressure to rotatory power, and there is an urgent demand for the blade to have light-weight and secure durability [1]. The wind turbine blade has a shape of the cantilever and is assembled into the main body of the wind power generator through a hub, and thus it should support enormous bending moment and torsional load as well as resisting extreme loads such as a squall. Accordingly, it results in the structural and functional damage to the whole wind power generator. Whereas, a light wind turbine blade, which is a thin composite plate consisting of core cells and outer tubes, can maintain enough structural strength.

For the external shape of the wind turbine, the NACA airfoil used in aircraft was selected as the blade model since their aerodynamic behavior is similar with each other. However, unlike the structure of the wing of aircraft, its inside is reinforced very simply with core cells. Accordingly, important design variables are the shape, number, installation location and thickness of the core cells. These design variables exert great effects on the structural strength and durability of the

whole wind turbine blade. Accordingly, much research has been conducted on methods of achieving highly energy efficient wind turbine blades through fluid analysis and design optimization of the blade.

Sorensen and Zahle performed fluid analysis on the slip stream flow at the back of the wind turbine blade by adjusting the mesh sizes of the analysis domain based on a $k-\omega$ Shear stress transport (SST) turbulent model [2]. Wubou and Hahm found the fluid velocity and turbulence intensity of the flow near the wind turbine blade using three-dimensional (3-D) Large Eddy simulation (LES) [3]. Kim et al. performed fluid analysis on the flow on the surface of a 1 MW wind turbine blade [4]. Kim et al. also optimized the shape of the airfoil to accord with the length of its chord [5]. Kwon et al. optimized the design of the blade such that its lift-drag ratio is maximized using fluid structure interaction analysis [6]. The studies cited above conducted research on the wind turbine blade using fluid analysis of the flow around the blade or optimized the exterior shape of the blade. In contrast, our aim is to optimize the inner structure of the blade by changing the thickness of the inner supporting structures on three cross sections of the blade, which is in line with the current design process of blades.

This study conducted as shown in Fig. 1 aerodynamics analysis on airfoil model DU25-A17 in order to figure out the optimum shape of the shear web structure on the section of the wind turbine blade and then performed topology optimization based on the result. In the aerodynamics analysis, to gain the pressure distribution on the surface of the blade, under the

*Corresponding author. Tel.: +82 51 510 2306, Fax.: +82 51 514 7640

E-mail address: oklim@pusan.ac.kr

[†]Recommended by Associate Editor Chang-Wan Kim

© KSME & Springer 2017

condition of cut-out wind speed with 25 m/s, two-dimensional CFD analysis was conducted by using the turbulent fluid flow as the FLUENT which passes through the transonic airfoil with the attack angle as 5° . In order to apply the inputted data calculated as the result of the aerodynamics analysis as the load data at the topology optimization of structural analysis, this study used the FSI mapping function internalized in the FLUENT and transmitted the result to OptiStruct, a program commercially used to conduct topology optimization. The load boundary condition for the topology optimization is applied as the nodal load of the mesh transcribed after the aerodynamics analysis in the fluid-structural coupled analysis, and the displacement boundary condition was analyzed with the inertia relief condition to deduce an optimum design plan of the core cell, the internal reinforcement structure of the blade.

2. Fluid analysis

2.1 5-MW Wind turbine blade

Fig. 2 is a 3-D model of the 5 MW wind turbine blade. As can be seen, its cross-sectional area changes from the root to the tip in a longitudinal direction. Fig. 3 is the cross section of the roof of the blade, composed of outer skin and inner supporting layers, such as leading edge spar, trailing edge spar, and shear web crossing the skin structure. The specifications for this 5-MW wind turbine blade are given in Table 1 [6].

Fiber reinforced polymer composites are usually used instead of metal to make large wind turbine blades. Fiber reinforced polymer composites such as glass fiber composites have low specific strength (strength/density) and specific modulus (modulus/density); consequently, they are widely applicable to problems requiring weight reduction [7]. The most commonly used materials are Glass Uni-directional (UD) material, Glass epoxy, Balsa wood, and PVC form.

This study applied only single material properties without considering the stacking design for composite materials. Glass UD material and high strength Glass epoxy are used for the outer skin and the inner structures, respectively. Detailed material properties are given in Table 2.

2.2 Fluid analysis of the wind turbine blade

The airfoil model of the 5 MW wind turbine blade is DU25-A17, which is the largest variable cross section among various airfoil models. The fluid analysis was carried out using FLUENT, with cut-out wind speed 25 m/s and attack angle 5° . The air flow surrounding the airfoil model was assumed to be a compressive and turbulent flow using $k-\omega$ SST [8], and the inner area was fixed using wall condition. As shown in Fig. 4, the leading and trailing edges were subjected to tensional pressure, while the suction and pressure sides were subjected to compressive pressure.

2.3 Topology optimization

Topology optimization is distinguished from both parameter

Table 1. Specifications for the 5 MW wind turbine blade.

Rating	5 MW blade
Rotor orientation, configuration	Upwind, 3 blades
Rotor diameter (m)	126
Hub diameter (m)	3
Cut-in wind speed (m/s)	3
Rated rotor speed (m/s)	11.4
Cut-out wind speed (m/s)	25

Table 2. Material properties for the 5 MW wind turbine blade.

Material	Density (kg/m ³)	Young's modulus (GPa)	Poisson's ratio
Glass UD mat.	1955	42.5	0.24
Glass epoxy	1872	8.1	0.27

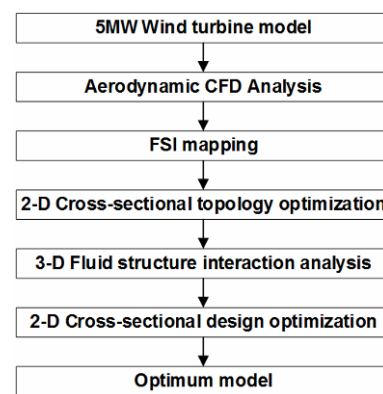


Fig. 1. Design procedure for the optimization of 5MW wind turbine blade.

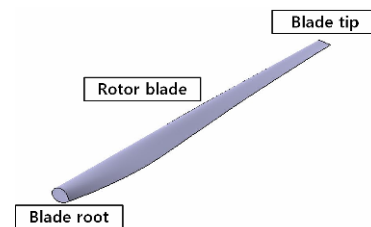


Fig. 2. 3D model of the 5 MW wind turbine blade.

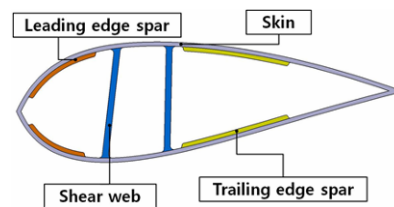


Fig. 3. Cross-section of the wind turbine blade.

and shape optimization methods because it seeks the optimum material distribution within a design domain for a given material boundary, loading or constraint conditions [9]. In the finite element-based topology optimizations, the design domain is

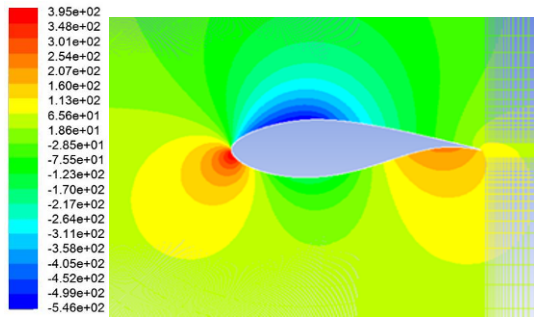


Fig. 4. Fluid analysis result for the DU25-A17 airfoil.

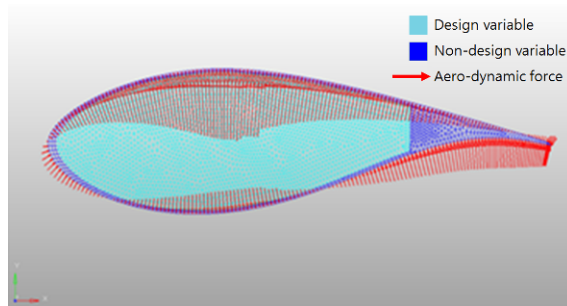


Fig. 5. Design domain and non-design domain of the blade.

commonly divided into a finite number of elements and the optimum material topology by selectively excluding the elements which do not have a significant effect on bearing the applied load [10, 11]. Because it is important to find the inner structures of the blade in order for it to endure extreme load conditions, topology optimization of its inner structures was carried out using fluid analysis to obtain the loading condition for topology optimization. The commercial optimization software, Optistruct version 11, was used. The results obtained from fluid analysis of the airfoil were used as load conditions for topology optimization. The inertial relief condition was used as the boundary condition to restrain the 2-D model and eliminate its rigid body motion. The 2-D blade model is divided by design domain and non-design domain to maintain its outer shape, as shown in Fig. 5.

The densities of all elements in the design domain are considered design variables. The upper and lower bounds of these design variables are one and zero, respectively. Fig. 6 shows the optimized density distribution of all elements. Two supporting structures were generated in the design domain. It was discovered that the inner supporting structures are important to enable endurance of load conditions occurring because of wind load.

3. Fluid structure interaction analysis

3.1 Analysis model

Following the acquisition of a 2-D blade model from the topology optimization, a detailed design needs to be generated. In this section, the Fluid structure interaction (FSI) analysis carried out to determine the stress distribution in the inner

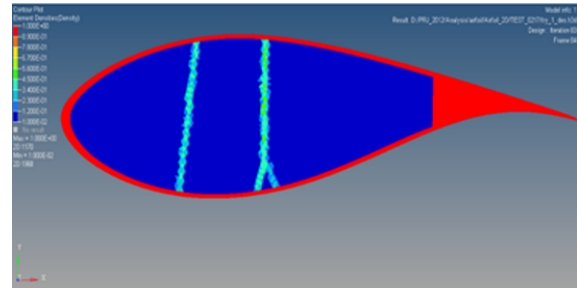


Fig. 6. Result of topology optimization.

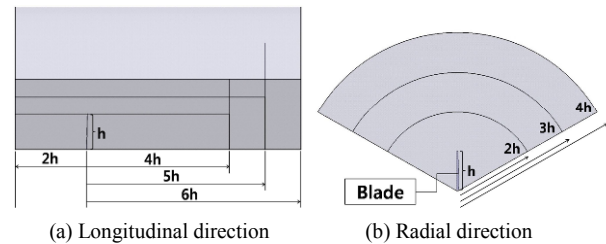


Fig. 7. Flow field models.

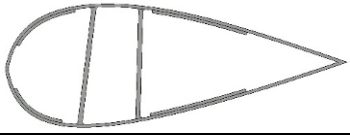
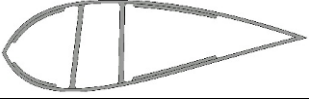

structure of the blade model due to loading conditions is outlined. There was no need for continuous repeated calculations of fluid dynamics due to structural changes in the airfoil shape because this study aimed to perform the optimization of the shear web structure for wind turbine blades. Thus, this study performed only one-way FSI. The fluid analysis results obtained in Sec. 2.1 are used as the load condition in this FSI analysis.

The analysis domain of a 3-D wind turbine blade model can be divided by structural models of three blades and flow fields surrounding the blades. The larger the size of the analysis domain of the flow field is, the more accurate the analysis results are. In general, the analysis domain of the flow field is generated to be much larger than the blade model. For example, the width and the height of the analysis model for the flow field are five and 10 times larger than the blade model, respectively. In real 5 MW blade models, the height of the blade is 61.5 m, and thus, the analysis domain is quite large, which requires much computational time.

Thus, fluid analysis of flow fields with various domain sizes is necessary to determine an appropriate domain size in order to reduce the computational time for the fluid analysis. Because the symmetry of the blade model is in a radial direction, one-third of the total model, including one blade, was used.

Assume that the overall length of the blade is h , as shown in Figs. 7(a) and (b). Assume that the lengths of the upper streams in the flow field, $2h$, $4h$, $5h$ and $6h$, are used as the lengths of the downstream in the longitudinal direction of the flow field. Likewise, $2h$, $3h$ and $4h$ are used as the radius of the flow field. Accordingly, fluid analysis of nine (3×3) models were performed. As a result, when the radius is larger than $3h$ and the length of the downstream is greater than $5h$, the analysis results were the same. Thus, the radius of the flow field was selected as $3h$, and the lengths of the upper stream

Table 3. Cross sections of the blade.

Section	Cross-sectional model
Sec. 1 (Root)	
Sec. 2 (Middle)	
Sec. 3 (Tip)	

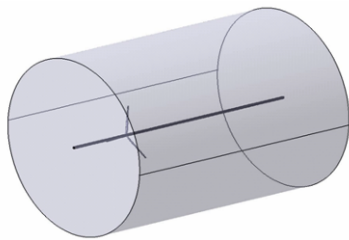


Fig. 8. Flow field model.

and downstream were selected as $2h$ and $5h$, respectively, as shown in Fig. 8.

The 2-D analysis models were extracted from the cross sections of the blades positioned at 16.25 m, 32.5 m and 48.75 m from the blade roof. On the basis of the optimization topology results obtained for the three cross sections, two spar webs were generated—the same as the cross sections of the real blades, as shown in Table 3.

3.2 3-D Fluid structure interaction analysis

In this section, we outline the analysis conducted on the air flow surrounding the blade using FLUENT to ascertain its influence on the blade. The meshes were generated using 10-node tetrahedral elements having intermediate nodes. On the region of the blade with high velocity and high pressure gradient, fine meshes were used to improve the accuracy of the analysis results. The inlet velocity and rotational speed of the blade were set to 12 m/s and 12.1 rpm , respectively, as boundary conditions of the 3-D fluid flow analysis. $K-\omega$ SST was used as the turbulence model because it is suitable for external fluid flow analysis. Owing to difficulty analyzing the air flow surrounding rotating blades, the Multiple reference frame (MRF) condition was used by rotating the flow field where the blade is fixed.

As shown in Fig. 9, the pressure increased from the root to the tip on the pressure side, and decreased from the roof to the tip on the suction side. This is because the fluid flow on the root has a slower flow recovery rate than the one on the tip.

Table 4. Force reaction.

Classification	Force reaction (N)		
	X	Y	Z
Sec. 1	217400	27551	5257
Sec. 2	165560	11374	4291.5
Sec. 3	91185	-1510.3	2390

Table 5. Moment reaction.

Classification	Moment reaction (N·mm)		
	X	Y	Z
Sec. 1	-3.0406e+008	5.5552e+009	1.5156e+008
Sec. 2	2.6146e+008	2.6369e+009	8.2606e+007
Sec. 3	2.8584e+007	7.174e+008	2.1797e+007

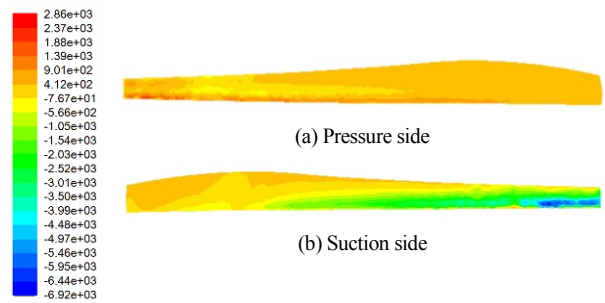


Fig. 9. Pressure contour.

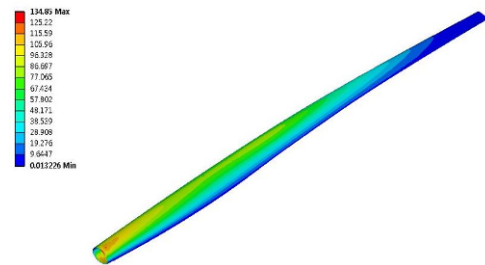


Fig. 10. Result of FSI analysis of the 5 MW wind turbine blade.

Three-dimensional FSI analysis was performed to determine the strength components generated inside the wind turbine blade by applying the fluid flow analysis results as load conditions. Because the wind turbine blades do not have a significant effect on the air flow, One-way FSI was used. Glass UD material, which has a relatively high mechanical strength and is commonly used, was chosen as the material for the blade. The pressure distribution obtained from the fluid flow analysis was applied to the load condition on the blade model for structural analysis. All degrees of freedom were fixed on the engaged area of the blade and its hub.

The maximum stress occurred on the root of the blade, which is quite similar with the destroyed blade region in real

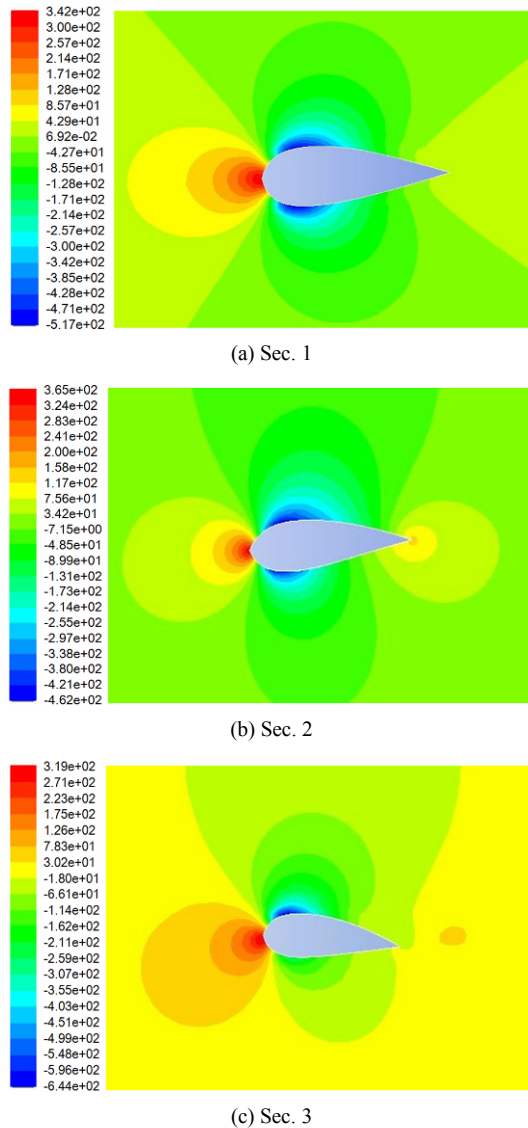


Fig. 11. Fluid analysis results.

cases. Using the results of the 3-D FSI analysis, the reaction force and the moment occurring in the inner structure of three cross sections were obtained, as shown in Tables 4 and 5.

3.3 2-D Fluid structure interaction analysis

Two-dimensional FSI analysis was also performed using the inner force obtained from the 3-D FSI analysis of the wind turbine blade. Analysis of the three sections shown in Fig. 6 was carried out by applying the aerodynamic loads and internal force as load conditions.

The inlet wind velocity was 25 m/s, and the attack angle was 5°. The turbulence model was k- ω SST, which is suitable for external fluid flow analysis. In order to ascertain the pressure distribution on the cross-section of the wind turbine blade, we assumed that the blade region was in the domains as a wall. The fluid flow analysis was performed by using the pressure based coupled solver. As shown in Fig. 11, the leading edge of

Table 6. Design variables.

Component	Lower bound	Upper bound	Thickness (mm)	Remarks	Design variable
Skin	15.73	44.27	30	①	X_1
Front shear web	23.59	66.41	45	②	X_2
Rear shear web	23.59	66.41	45	③	X_3
Leading edge spar	15.73	44.27	45	④	X_4
Trailing edge spar	15.73	44.27	30	⑤	X_5

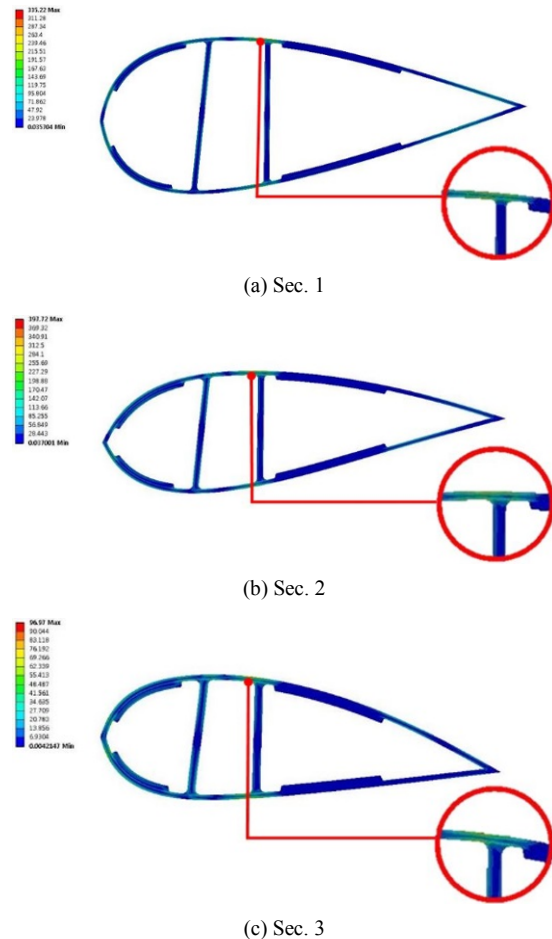


Fig. 12. FSI analysis results.

the cross section was under compressive pressure, and the trailing edge was under tensional pressure.

On the basis of the fluid flow analysis results, we conducted structural analysis of the 2-D cross section. The pressure data obtained from the flow analysis was applied as input loads at the external mesh of skin. The reaction forces and moments of the internal blade obtained from the 3-D FSI analysis were applied at the center of gravity of the cross section. The displacement boundary conditions were defined as inertia relief (free-free) conditions.

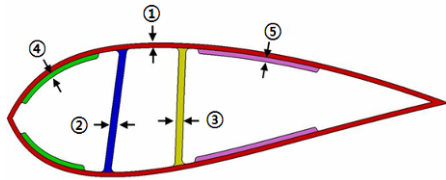


Fig. 13. Selection of design variables.

Fig. 12 is the FSI analysis results for the three cross sections. At Sec. 1, the maximum stress, 335.22 MPa, appeared at the top of the skin near the filleted area where the skin and web are combined. Likewise, the maximum stress at Secs. 2 and 3 were, respectively, 397.72 MPa and 96.97 MPa occurred in the same area. The maximum stresses at Secs. 1 and 2 are much greater than the yield stress (250 MPa) of the skin’s material properties, Glass UD material; therefore, structural design of the blade is necessary.

4. Design optimization

4.1 Formulation

In this study, the thickness of the skin, leading and trailing edge spars, and front and rear shear web were considered as design variables, as illustrated in Fig. 13. The bounds of the design variables were set to 20 % of the upper and lower limits. The maximum stress at each cross section (σ_{max}) was subjected to a smaller yield stress than that of the Glass UD material (σ_y). The objective function was used to minimize the area of the three cross sections, and the design optimization was formulated as Eq. (1):

$$\begin{aligned}
 & \text{Find} && \mathbf{X} = \{X_i\}, && i = 1, \dots, 5 \\
 & \text{to minimize} && A_c(\mathbf{X}) && (1) \\
 & \text{subject to} && \sigma_{max}(\mathbf{X}) \leq \sigma_y \\
 & && \mathbf{X}^L \leq \mathbf{X} \leq \mathbf{X}^U.
 \end{aligned}$$

For the optimization, 43 design points were used for Central composited design (CCD), and a response surface model was generated using the least square method. Direct research algorithm, the most efficient algorithm among the various optimization algorithms for area minimization, was selected, and Sequential two-point diagonal quadratic approximate optimization (STDQAO), which is based on approximate models and is an efficient algorithm, was selected as the optimization method.

4.2 Design optimization result for cross sections

The optimization results for the three sections are shown in Table 7. The values for all design variables in the initial model were significantly reduced to those in the optimum model. In particular, the thicknesses of the skin, rear shear web, and the

Table 7. Optimum design of Secs. 1-3.

Variables	Sec. 1		Sec. 2		Sec. 3	
	Initial design	Optimum design	Initial design	Optimum design	Initial design	Optimum design
X_1	30.00	15.73	30.00	15.73	30.00	15.73
X_2	45.00	25.04	45.00	30.14	45.00	23.59
X_3	45.00	23.59	45.00	23.59	45.00	23.59
X_4	30.00	26.14	30.00	24.15	30.00	16.40
X_5	30.00	15.73	30.00	15.73	30.00	15.73
Area	441490	251183	333426	192416	259914	141024
Stress	335.22	231.59	411.90	244.95	96.94	244.00

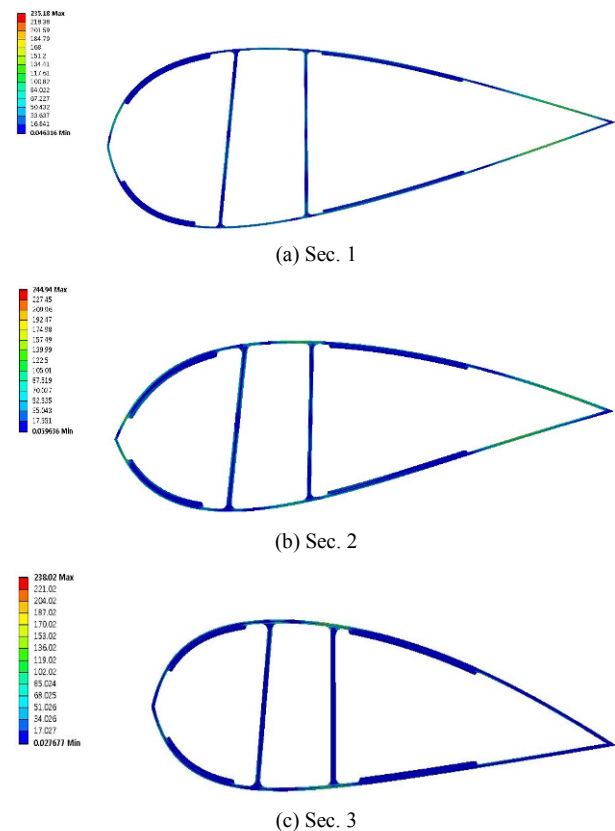


Fig. 14. Results of FSI analysis for optimized sections.

tailing edge spar converged to the lower bounds of the design variables in all sections. Because the leading edge spar is subjected to the pressure distribution caused by the air inflow and the front shear is subjected to the inner force and moments, those in the initial model converge to some specific values within their upper and lower bounds in the optimum model.

In Sec. 1, the area of the initial model was significantly reduced by 43 % because of the decrease in all dimension variables to satisfy the constraint for the maximum stress. In the optimum model for Sec. 1, the maximum stress occurs at the trailing edge, as shown in Fig. 14(a), unlike its occurrence at the fillet area between the upper skin and the rear web in the

initial model in Fig. 12(a). The stress concentration is severe at the fillet area of the initial model, and the maximum stress is greater than the yield stress of the glass UD material. On the other hand, the stress at the optimum model becomes mostly evenly distributed as the dimensions of all design variables decrease, and thus, the maximum stress becomes smaller than the yield stress of the glass UD material.

In Sec. 2, the thickness of the front shear web is much greater than that in Sec. 1 because the maximum pressure caused by the air inflow in Sec. 2 is greater than that in Sec. 1. Nevertheless, the thickness of the front shear web is still significantly reduced and other design variables have lower limits, and thus, the area is reduced by 42.4 %. Like the results for Sec. 1, the maximum stress occurs at the trailing edge of the blade. It is also significantly reduced by 40.5 % as the stress becomes evenly distributed in the overall section.

Sec. 3 is the closest section to the blade tip and its area is the smallest. Accordingly, Sec. 3 endures less inner force and moments than other sections, so that the thickness of the front shear web converges to the lower bound similar to the manner in which the thickness of skin, rear shear web, and trailing edge spar converge to their lower bounds. The area is reduced by 45.7 %, which is the largest reduction rate of all sections, and the constraint for the maximum stress is close to the yield stress of the glass UD material.

As a result of the optimization, the areas of the cross sections were significantly reduced, which resulted in them satisfying the constraints for the maximum stress occurring at the cross sections. The optimized cross sections can be used to generate a real 3-D blade model by interpolating the cross sections and creating a multi-section model that passes through them. The reduced area of the cross sections can significantly reduce the volume of the 3-D blade model, and thus, reduce the weight of the wind turbine blade and material cost.

5. Conclusions

In this study, the cross sections of a 5 MW wind turbine blade were optimized through topology optimization, fluid analysis, and 3-D and 2-D FSI analysis.

First, topology optimization was performed to find the inner structures of the cross section of the wind turbine blade using 3-D fluid analysis of the air flow surrounding the blade. The inner structure of the blade obtained was then used as 2-D models for design optimization of the cross sections of the blade.

Next, 3-D FSI analysis was used to find reaction forces and moments occurring on the cross sections positioned at the root, middle, and tip of the blade. Two-dimensional FSI analysis was also performed to find the maximum stress on the cross sections, and it was found that design optimization of the cross sections is necessary.

Finally, design optimization of the three cross sections was performed and, as a result, the area of the blade and maximum

stress were significantly reduced. Accordingly, the material cost can be considerably reduced with satisfactory strength. Optimization of the cross sections was used to design real wind turbine blades, and thus, this approach and the results obtained can be very useful in designing real wind turbine blades.

Acknowledgment

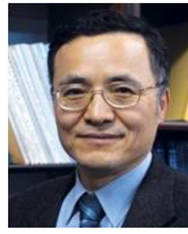
This research was supported by the Basic Science Research Program through the National Research Foundation of Korea (NRF) funded by the Ministry of Education (NRF-2012R1A1A2003675).

References

- [1] J. S. Choi, K. H. Kim and K. T. Lee, Preliminary analysis of the wind turbine requirements for domestic use, *Trans. The Korean Society for Aeronautical & Space Sciences*, 30 (1) (2002) 165-172.
- [2] N. Sorensen and F. Zahle, On the influence of far-wake resolution in wind turbine flow simulations, *Journal of Physics: Conference Series*, 75 (2007) (012042).
- [3] S. Wubou and T. Hahm, 3D-simulation of the turbulent wake behind a wind turbine, *Journal of Physics: Conference Series*, 75 (2007) (012033).
- [4] B. S. Kim, M. E. Kim and Y. H. Lee, Basic configuration design and performance prediction of a 1MW wind turbine blade, *Journal of Fluid Machinery*, 11 (5) (2008) 15-21.
- [5] S. Y. Kim, B. S. Kim, J. H. Kim, C. D. Nam and Y. H. Lee, A study on optimum design of turbine blade for wind power generation, *Proc. of the KSME 2002 Spring Annual Meeting*, 2002 (4) (2002) 112-117.
- [6] H. I. Kwon, D. O. Ryu, J. Y. Yoo and O. J. Kwon, Aerodynamic sectional design optimization of wind turbine rotor blade considering elastic structural deformation, *Proceedings of KSAS-JSASS Joint International Symposium on Aerospace Engineering*, 2011 (11) 1276-1283.
- [7] Y. S. Kim, A study on the characteristics of generation technique using renewable energy, *M.S. Thesis*, Chosun University, Korea (2002) 9-12.
- [8] G. P. Corten, *Inviscid stall Model*, EWEC, Copenhagen (2000) 466-469.
- [9] C. S. Cho, E. H. Choi, J. R. Cho and O. K. Lim, Topology and parameter optimization of a foaming jig reinforcement structure by the response surface method, *Computer-Aided Design*, 43 (2011) 1707-1716.
- [10] Y. Fu and X. Zhang, An optimization approach for black-and-white and hinge-removal topology designs, *Journal of Mechanical Science and Technology*, 28 (2) (2014) 581-593.
- [11] D. Xiao, H. Zhang, X. Liu, T. He and Y. Shan, Novel steel wheel design based on multi-objective topology optimization, *Journal of Mechanical Science and Technology*, 28 (3) (2014) 1007-1016.



Dong-Hoon Kim received his B.S. and M.S. degrees in Mechanical and Automotive Engineering from Keimyung University in 2013 and 2015, respectively. Kim is currently worked at the Research and Development Center Test and CAE Team, HWASHIN Co., LTD.



O-Kaung Lim received his B.S. degree in Mechanical Engineering from Seoul National University in 1972 and M.S. degree in Mechanical Engineering from KAIST in 1976, respectively. He then received his Ph.D. degree from University of Iowa in 1982. He served as a Head of the School of Mechanical Engineering in Pusan National University. Dr. Lim is currently a Chair of the Innovation Center for Engineering Education in Pusan National University. Dr. Lim's current research interests include education methodology for engineering design and nonlinear optimization.